



Laser-Based Ultrasonics: Applications at APL

David W. Blodgett and Kevin C. Baldwin

Conventional ultrasonic techniques have long been recognized for their usefulness in the nondestructive testing of materials and structures. These techniques, based on launching ultrasonic or high-frequency acoustic waves into a material using a coupled transducer, enable the probing of certain material properties. By inducing surface or bulk waves into a material, several material properties, such as thickness, layer structure, and elastic moduli, can be measured. In addition, the material can be checked for cracks, delamination, or changes in porosity. Thus, by launching waves into a material and detecting any corresponding acoustic wave arrivals, it is possible to determine a significant amount of information about the material under test. In contrast to conventional methods, the field of laser-based ultrasonics (LBU) allows the same information to be collected, but through noncontact methods. In this article, we highlight the use of LBU to address problems relevant to air defense, space, and biomedicine.

INTRODUCTION TO LASER-BASED ULTRASONICS

Ultrasound and Conventional Ultrasonic Testing

The generation and detection of ultrasonic waves is one way of characterizing the bulk (interior) and surface properties of a material. Up to three bulk acoustic waves, one longitudinal and two transverse shear, can be supported, each with its own characteristic velocity.^{1,2} As an ultrasonic wave propagates, its amplitude decreases because of geometrical spreading, attenuation from absorption in the medium, and scatter from discontinuities. Measurement of these propagation characteristics provides insight into the bulk properties of the material. A list of the material properties that can be determined using ultrasonics is provided in Table 1.

In addition to bulk wave propagation, acoustic waves traveling along the surface of the material can also be generated. From surface-wave velocity measurements, information concerning surface texture, residual stress, and the thickness and quality of surface treatments can be gained.²

Conventional ultrasonics use a contact transducer for both the generation and detection of various ultrasonic wave types. Proper coupling of these transducers to the material is required to ensure a reasonable level of sensitivity. In addition, the transducers tend to be relatively large, with typical diameters on the order

Table 1. Application of ultrasonics to material property measurements.

Property	Measurements
Dimensional	Thickness and density
Compositional	Impurity levels
Microstructural	Grain size, anisotropy, number, and distribution of phases
Mechanical	Elastic moduli
Inspection	Defects, discontinuities, interfaces, and bonds

of 0.25 to 1.00 in. These coupling and size requirements often make their use problematic.

Laser-Based Generation of Ultrasound

Laser-based ultrasonics (LBU) is a technique that uses laser sources to generate and detect high-frequency ultrasound. Generation is accomplished by illuminating a sample with a short-pulse laser. The laser energy absorbed by the sample causes localized heating, with accompanying thermal expansion. Absorption of the incident pulse energy and the associated temperature gradients induces a rapidly changing strain field. This strain field, in turn, radiates energy as elastic (ultrasonic) waves.²⁻⁴ At low pulse power, this is an entirely thermoelastic process resulting in no damage to the sample. The effect is similar to what would be expected from a mechanical impact; i.e., a traveling acoustic wave is generated that propagates both through and along the sample, producing very small deformations in the surface (a few nanometers) when it reaches a boundary.

The efficient generation of ultrasound depends on the material's absorption characteristics at the optical wavelength of the pulsed laser. Therefore, two different pulsed laser systems are often used: an Nd:YAG laser (1.064 μm) and a CO₂ laser (10.600 μm). The Nd:YAG laser is typically used when working with metals and composite materials, whereas the CO₂ laser is best suited for glasses and ceramics.

Laser-Based Detection of Ultrasound

Optical interferometry provides a complementary noncontact technique for the measurement of acoustic wavefront arrivals.^{2,5} As previously stated, small displacements at the sample surface occur because of the arrival of the elastic wavefronts (longitudinal or shear) at a boundary. By using the sample surface as a mirror in one arm of a Michelson-type interferometer, the output signal of the interferometer can be used to measure both the arrival time and amplitude of the surface displacement.^{5,6} A simple schematic of an LBU system is shown in Fig. 1.

The notable advantages and disadvantages of LBU, when compared to conventional transducer-based ultrasonics, are captured below.⁷ Advantages include

- Noncontact (couplant problems eliminated and no surface loading)
- Remote (access to sample in hostile environments)
- Rapid scanning capability
- Allows operation on geometrically awkward specimens
- Can be used as an ultrasonic point source (both temporally and spatially)
- Broadband (UHF generation and detection possible)
- Reproducible source
- Laser interferometry offers an absolute calibration standard
- Generation of both surface and bulk acoustic waves
- Shaping of ultrasonic surface wavefronts (by controlling the spatial distribution of the source)

Disadvantages include

- Sensitivity (optical techniques generally have lower sensitivity than other methods)
- Relatively expensive
- Generation efficiency is a function of material optical absorption properties
- Requires laser safety precautions

The Role of LBU at APL

As the lists above suggest, LBU is not the solution to every material characterization problem; sometimes the quickest and easiest thing to do is to just place a transducer on the sample. But the approach truly depends on what is being tested and the environment under which it is being tested. In this article, we highlight three cases in which the use of conventional ultrasound would have proved difficult or inapplicable and

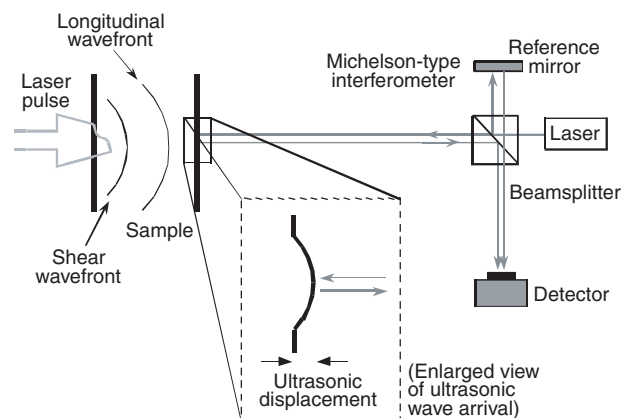


Figure 1. Ultrasonic measurement scheme using a pulsed laser for ultrasound generation and a Michelson-type interferometer for ultrasound detection.

LBU was able to supply the needed measurements. Specific applications developed and tested at APL include determination of the effects of bulk treatments on the high-temperature elastic moduli of sapphire, inspection of thin solar panel structures for spacecraft applications, and the *in vitro* assessment of tooth health.

ELASTIC MODULI AND DEFECT ORIENTATION STUDIES OF PROCESS-TREATED SAPPHIRE

Motivation

Of interest to the missile community is the high-temperature mechanical behavior of optical window materials. For IR transparent windows in endo-atmospheric missiles, single-crystal sapphire is the material of choice.⁸ However, sapphire has been found to undergo a significant drop in mechanical properties at high temperatures, leading to a potential fracture of the window under typical flight conditions. In an effort to delay the onset of fracture in single-crystal sapphire, several bulk treatment processes have been investigated.⁹ It was hoped that by introducing defects into the crystal structure, twin propagation would be impeded. Of importance, then, was whether these defects would also affect physical properties such as the elastic moduli.

As the name suggests, the elastic modulus of a material is a parameter similar to that of the restoring constant of a spring. It relates the amount of strain (deformation) that a material will experience when placed under a particular stress (force). Thus, knowledge of the elastic modulus is important for understanding how the material will respond to mechanical loads or thermal gradients. In particular, the behavior of the modulus as a function of temperature is critical because it enables prediction of the stress levels within a sensor window as it is heated during flight.

Single-crystal sapphire displays trigonal symmetry, requiring the determination of six unique elastic moduli: C_{11} – C_{14} , C_{33} , and C_{44} .^{10,11} Figure 2 shows the crystal symmetry of sapphire using the conventional rectangular coordinate system, where a , c , and m are the primary axes. The r -axis is in the c – m plane, inclined at 32.4° from the m -axis.

Measurement of the wave velocities along each of the crystallographic directions enables the determination of all six elastic moduli.¹⁰ To obtain all six, two sets of four specifically oriented sapphire samples were cut. One set of four was process treated and the other provided the control for comparison. Each set of four samples was 1.5 in. in diameter and 3/8 in. thick, with the a -, c -, m -, and r -axis oriented perpendicular to the face of the sample.

Measurement of the arrival times for each of the ultrasonic waves, coupled with knowledge of the sample

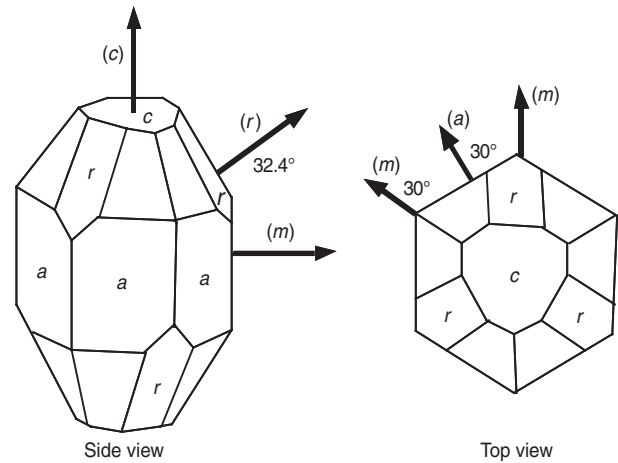


Figure 2. Crystallographic symmetry of single-crystal sapphire.

thickness, allowed the respective wave speeds to be determined. For example, propagation of a stress wave along the c -axis yields two characteristic wave velocities, one pure longitudinal and one pure shear (due to degeneracy):

$$v_1 = \sqrt{\frac{C_{33}}{\rho}} \quad (1)$$

and

$$v_2 = \sqrt{\frac{C_{44}}{\rho}}. \quad (2)$$

This allows the direct determination of C_{33} and C_{44} based on directly observed wave speeds and knowledge of the material density ρ . Many of the remaining formulations of the moduli are much more involved and based on other measured wave velocities and other previously calculated moduli. They are not repeated here.

The determination of the elastic moduli of a material from wave speed measurements using ultrasonic methods is well documented.^{12,13} Traditionally, these measurements were performed using a contact transducer to both generate and detect the ultrasonic wave arrivals.² However, the maximum temperature for contact ultrasonic measurements is limited both by the couplant used between the transducer and the material and, ultimately, by the Curie temperature of the transducer. Papadakis et al.¹⁴ were able to extend the maximum temperature of these measurements to 1200°C by using a momentary contact technique. In this configuration, a long, cool buffer rod is placed in momentary contact (≈ 100 ms) with the sample. A contact transducer mounted to the end of this buffer rod is then used to both transmit the ultrasonic signal and receive the echo.

Application of LBU

As mentioned earlier, the purpose of the present study was to determine if there is a change in the mechanical strength of process-treated sapphire as a function of temperature.^{15–21} The noncontact nature of LBU allows the sapphire samples to be placed in a high-temperature furnace and then heated to the desired temperature. The furnace used here is capable of temperatures approaching 1700°C.

Figure 3 shows the typical LBU waveforms, taken at room temperature, for each of the crystallographic orientations. The arrival times used to determine the wave speeds and the elastic moduli are marked on the waveforms. For example, the *c*-axis waveform shows the longitudinal wave arrival at time t_1 and the shear wave arrival at time t_2 . Use of Eqs. 1 and 2 allows C_{33} and C_{44} elastic moduli to be calculated as 496 and 145 GPa, respectively (assuming a density of 3.98 g/cm³).

Measurements of wave speed were taken at 25°C increments so that a complete picture of the temperature dependence of the elastic moduli could be determined. Shown in Fig. 4 are plots of the acoustic wave speeds for untreated sapphire with a corresponding curve fit. These curve fits were used in subsequent calculations for the elastic moduli. Similar curve fits were obtained for the wave speeds of the treated sapphire.

Analysis and Results

Curve fits for two of the elastic moduli, as determined using the LBU technique, are plotted in Fig. 5 as a function of temperature. Values published by Goto et al.²² have been overlaid on the figure for reference. Excellent agreement is found between the published values and those for the untreated sapphire. A 1% drop in the C_{11} modulus for the treated sapphire compared to the untreated sapphire was found. The largest discrepancies between the untreated and treated sapphire samples were found for C_{12} and C_{14} . These discrepancies may

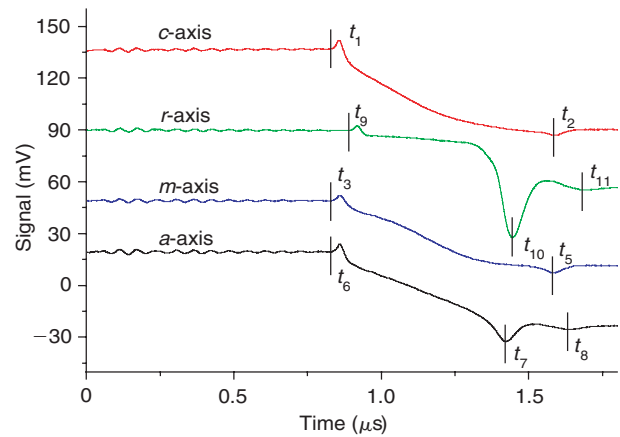


Figure 3. Room-temperature ultrasonic waveforms in untreated sapphire for the four crystallographic orientations.¹⁸

help explain differences in the measured biaxial and four-point flexure strength.²²

INSPECTION OF SOLAR PANEL COUPONS FOR SPACEFLIGHT HARDWARE

Motivation

After thermal cycling of the MESSENGER (<http://messenger.jhuapl.edu>) flight panels, approximately one in four of the solar cells populating the flight-ready panel exhibited a hazing effect near the center of the cell.²³ The solar panel sections are composed of 18 solar cells, each covered by a thin, protective glass substrate cemented to the solar cell with a droplet of epoxy. The visible hazing appeared to correlate well with the location of a droplet, raising concerns that the protective glass cover slip may be disbonding from the substrate. Note that the purpose of this study was not to quantify any disbond present, but rather to examine the mechanical properties of the

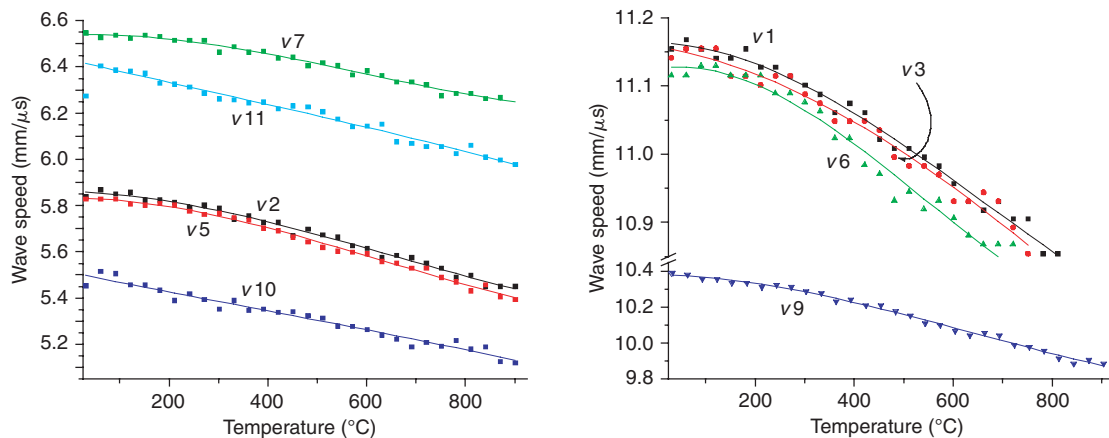


Figure 4. Measured temperature dependence of the ultrasonic wave speeds for the untreated sapphire samples (with curve fit).¹⁸

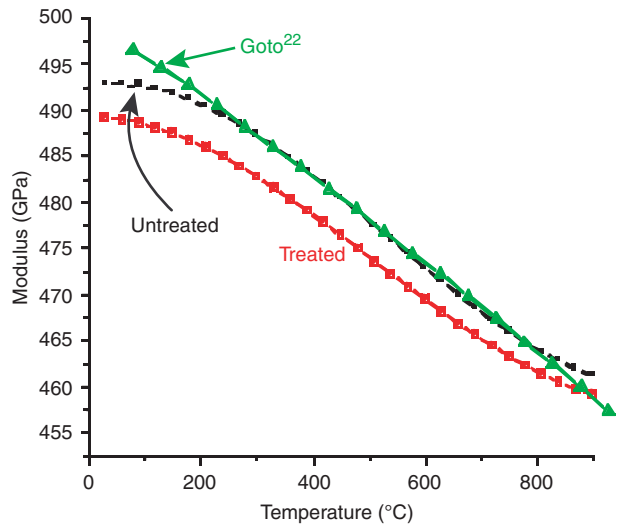


Figure 5. Comparison of the temperature dependence of the elastic moduli for untreated, treated, and published²² results for C_{11} .

assembled cells for any anomalies that would indicate a potential problem meriting further investigation.

Application of LBU

As mentioned previously, laser-generated ultrasound results in both bulk and surface acoustic waves. As opposed to the previous application, in which the velocity of bulk waves was used to determine the elastic moduli of a material, surface waves were used to probe the layered solar cell structure. A cylindrical lens focused the laser pulse to a line source and efficiently generated surface acoustic waves perpendicular to its axis (Fig. 6). The width of the laser line profile determined the frequency (wavelength) content of the launched surface wave and controlled the depth at which the acoustic wave interacted with the sample.^{2,7}

Both aspects of the generation were important for exploring the solar panel bonding problem. By controlling the width of the generation spot, the thickness corresponding to the upper and lower epoxy joints could be interrogated. Noticeable decreases in signal amplitude and frequency content through these regions could be used to determine the strength of the mechanical bond because poor bonds correspond to high attenuation and result in low-pass signal filtering.

High-frequency ultrasonic waves were generated in the glass cover slip using a pulsed CO_2 laser ($10.6 \mu\text{m}$). The CO_2 laser was chosen here because the laser wavelength corresponds to a region of high absorption of the protective glass substrate. Again, at low pulse powers, this is a completely nondestructive process. A high-bandwidth laser vibrometer (Polytec OFV-353) was used to detect the resulting surface velocities, which were induced by the displacements caused by the propagating surface wave approximately 2 cm from the generation location.

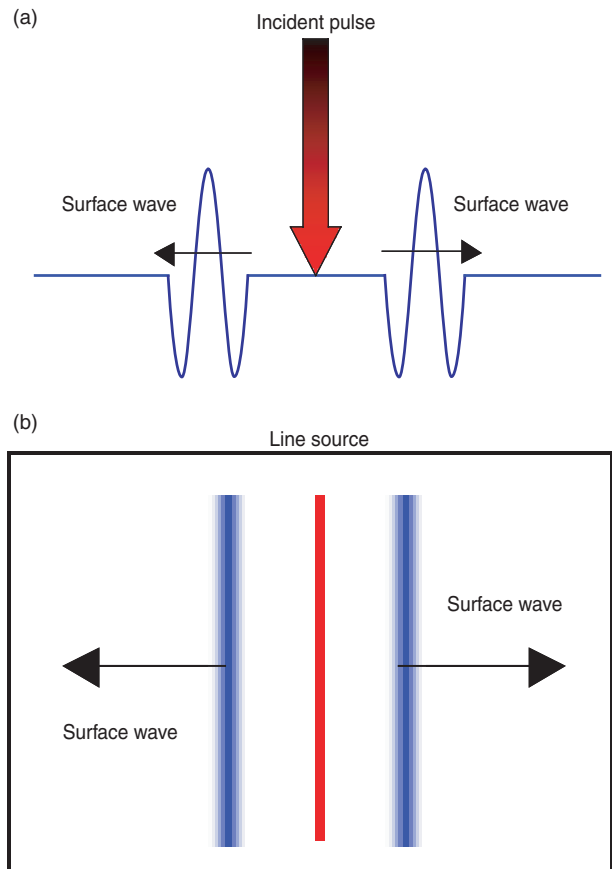


Figure 6. Generation of surface waves. (a) Side view, indicating that the acoustic surface wave penetrates into the material as a function of amplitude. (b) Top view, indicating the directionality of the surface wave generated by a laser line source.

Two spatially distinct reflections (air/glass and adhesive/solar cell) resulted from illuminating the solar cell with the vibrometer laser, providing a unique measurement opportunity (Fig. 7). By selecting which reflection to use for velocity (displacement) measurements, the acoustic waves traveling along the front surface of the glass (first reflection) or the substrate (second reflection) could be measured independently.

Analysis and Results

Four test coupons were measured: a severely hazed cell, a moderately hazed cell, and two nominal cells. When waveforms from the two reflections from a single coupon were compared, the waveforms from the good samples showed high correlation. However, the waveforms from the moderately hazed cell were less correlated, and those from the severely hazed cell were quite noticeably uncorrelated. These results, shown in Fig. 8, suggested that there was a disbonding of the glass cover slip from the substrate layer for the hazed cells, whereas cells that showed no hazing effect were well bonded. The increased decorrelation of the waveforms, as a function of hazing, was attributed to greater degrees of

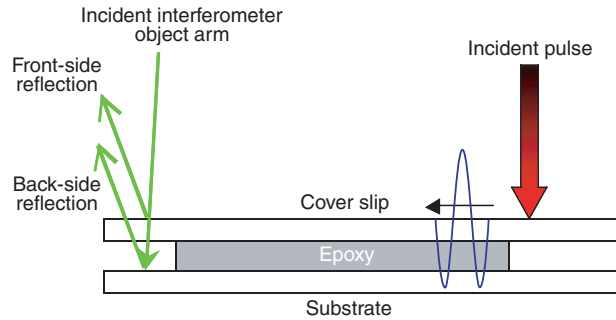


Figure 7. Laser ultrasound generation and detection on a solar cell.

attenuation of the higher-frequency surface acoustic waves as they propagated across the disbonded region.

In this case, LBU was able to provide considerable insight into the situation within a very fast turnaround time. Laser-based generation and detection were well suited for this particular application because of the small interrogation region and nondestructive nature of the measurements. These measurements indicated that the observed hazing effect, and the possible effect on the mechanical properties of the cell, merited further study.

ASSESSMENT OF TOOTH HEALTH

Motivation

Dental health care and research professionals require a means of imaging the structures within teeth *in vivo*. For example, there is a need to image the margins of a restoration to detect poor bonding or voids between the restorative material and the dentin. In addition, a high-resolution imaging modality is needed to detect tooth decay in its early stages. If decay can be detected early enough, the process can be monitored and interventional procedures, such as fluoride washes and controlled diet, can be initiated to help remineralize the tooth. Currently, X-ray imaging is limited in its ability to visualize interfaces and incapable of detecting decay at a stage early enough to avoid invasive cavity preparation followed by a restoration.

Dental enamel is the hard protective substance that covers the crown of the tooth. It is the hardest biologic tissue in the body and designed to resist fractures during mastication (chewing). Enamel is composed of about 96% inorganic mineral in the form of hydroxyapatite and 4% water and organic matter.^{24,25} Dentin is the hard tissue that constitutes the body of the tooth.

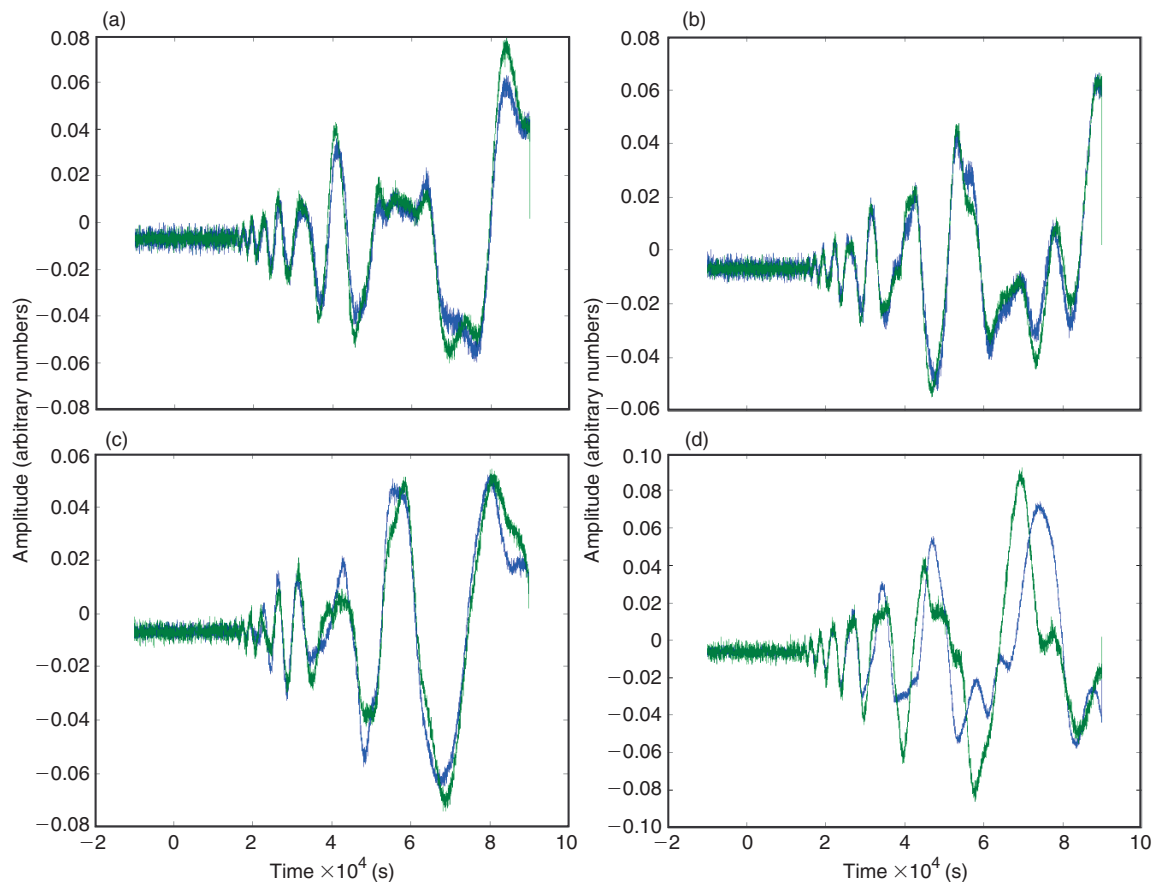


Figure 8. Ultrasonic waveforms measured on nominal solar cell coupons (a and b), a moderately hazed coupon (c), and a severely hazed coupon (d). The two waveforms in each plot are from the two different surfaces of the solar cell, the glass cover slip and the substrate layer.

Unlike enamel, which is almost white in color, dentin appears almost yellowish. Dentin is a living tissue that is not normally exposed to the oral environment. Like bone, dentin is composed primarily of an organic matrix of collagen fibers (20%), inorganic hydroxyapatite crystals (70%), and about 10% water.²⁵ With 20% less mineral than enamel, dentin is softer and slightly elastic.

Attempts to apply conventional ultrasonic techniques to the examination of the internal structure of a tooth have met with mixed success.^{26–29} One of the major obstacles is finding a suitable couplant for the transducer to the tooth for *in vivo* measurements. Without proper coupling, it is difficult to transfer acoustic energy into the tooth. Early investigators^{27,28} attempted to use water, as with soft tissue structures, but the results were not convincing. Reich et al.²⁹ overcame this problem by replacing water with mercury. Although providing superior coupling efficiency, mercury would never be suitable for clinical applications. Barber et al.²⁶ used a small aluminum buffer rod to transfer the acoustic energy from the contact transducer to the tooth. Although eliminating the coupling problem, the buffer rod required that

a small flat spot be ground in the surface of the tooth, making *in vivo* measurements impossible and limiting spatial resolution. Other researchers have attempted to use an acoustic microscope to characterize the properties of teeth^{30,31} to improve the spatial resolution of the measurements. However, as with the previous work by Barber et al.,²⁶ special polishing of the tooth samples was required, again making the technique ill-suited for clinical applications.

Laser ultrasonics overcomes the previous difficulties in coupling efficiency, surface preparation, and detection footprint size. Specifically, in Figs. 9 and 10, *in vitro* measurements are presented for sections of extracted human molars. These results are compared with those obtained on specially prepared tooth phantoms with mechanical interface properties similar to those found in teeth. In addition, results from extracted human teeth are presented to show that ultrasound is sensitive to the anisotropic and inhomogeneous nature of dentin, both within a single tooth and between different teeth. Finally, ultrasonic measurements are presented on an extracted human molar with a surface caries (cavity).

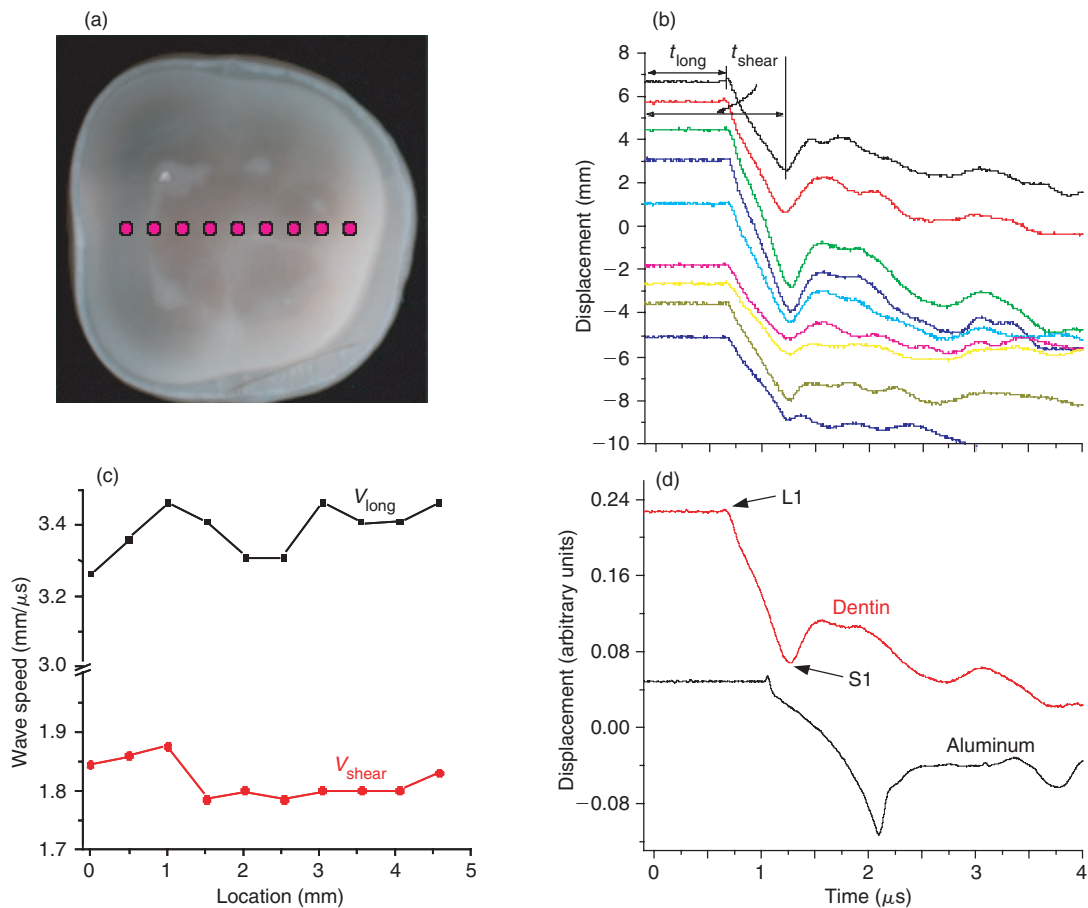


Figure 9. Variations in the acoustic wave speeds in dentin attributable to anisotropy and inhomogeneity were measured in specially prepared dentin sections. Shown in (a) is a picture of one of the dentin sections with the location of the ultrasonic measurements marked. Measured ultrasonic waveforms across the dentin section taken at 500- μ m intervals are shown in (b), with a plot of the calculated wave speeds shown in (c) and a comparison to an elastically isotropic material (aluminum) in (d).

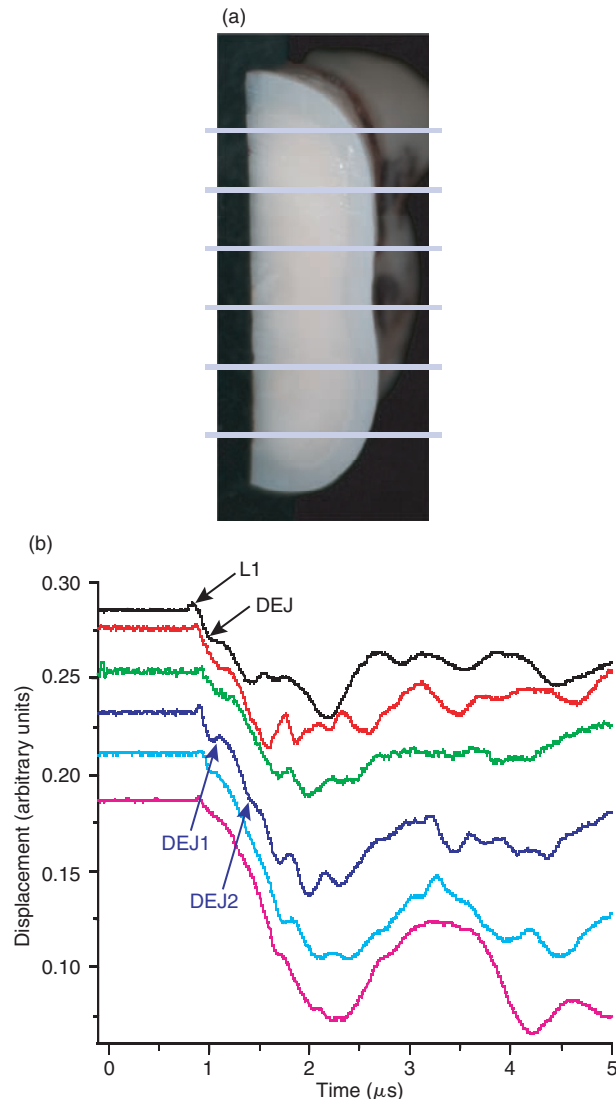


Figure 10. Variations in ultrasonic waveforms were measured in a section of extracted molar. (a) An image of the sectioned molar through which the ultrasonic measurements were made showing the dentin/enamel junction (DEJ). (b) Selected waveforms measured through the DEJ.³²

Application of LBU

Characterization of Bulk Properties

The interface properties of dental hard tissues were characterized on specially prepared sections of extracted molars.^{32–35} The first sets of molars were sectioned between the occlusal (top) surface and just above the pulp chamber. These sections were typically between 2 and 3 mm thick and allowed characterization of the acoustic properties of dentin. Figure 9a shows one of the extracted tooth sections (2.25 mm thick), with the enamel ring visible around the dentin. Measurements were taken across the middle of the section at 500- μm intervals. Shown in Fig. 9b are the measured ultrasonic waveforms taken from the left (top waveform) to right (bottom waveform) of the section. The first measurement was taken about 2 mm to the right of the enamel

to avoid boundary effects. The longitudinal and shear wave arrivals are marked in the top waveform. These waveforms are similar to those found for the elastically isotropic material, shown in Fig. 9d, where the first longitudinal L1 and shear S1 are marked. The corresponding calculated wave speeds are shown in Fig. 9c and vary less than 5% across the tooth section. More than 100 measurements were made from 10 different sections, and the average longitudinal and shear wave speeds were 3.35 and 1.83 mm/ μs , respectively. The total variation in acoustic wave speeds was found to be less than 10% over all of these measurements. The 10% variations are similar to those found by Lertchirakarn et al.³⁶ in their measurements of the ultimate tensile strength of dentin.

Additional measurements on an extracted molar sectioned through the apex of the tooth are shown in Fig. 10a. This tooth section allowed the interface properties at the dentin/enamel junctions to be characterized. For these measurements, the ultrasound was generated on the sectioned dentin side and the interferometric measurements on the “as-is” enamel surfaces. The corresponding measured ultrasonic waveforms are shown in Fig. 10b. These measurements were taken at 0.5-mm increments, starting about 1 mm below the enamel on the top portion of the tooth. In this region, the enamel and dentin are about 0.84 and 2.54 mm thick, respectively. Variations in waveforms were attributed to differences in both acoustic wave speeds and dental hard tissue thicknesses.

Identification of Caries

The effects of caries (or surface cavities) on surface waves were also studied. Dental caries are linked to the bacteria in plaque, which may produce acid that can cause etching and disintegration of the tooth’s surface. In these measurements, the source and receiver were maintained at a constant separation. Ultrasonic measurements were taken through, at the edge of, and below the caries (Fig. 11a). The time window, indicated in Fig. 11b, denotes the time during which the first surface wave arrives. This figure shows that very little acoustic energy propagates through the caries because of scattering by the surface disintegration. At the edge of and/or below the caries, there is a distinct surface wave arrival. The surface wave that propagates below the caries is the sharpest, indicating the least amount of scatter. To better characterize the amount of scatter, the frequency spectrum was generated over the windowed portion of each waveform; the resulting magnitude is plotted in Fig. 11c. These spectra clearly show the effects of porosity on wave propagation.

CONCLUSIONS

This article highlighted just a few example applications of laser ultrasonics at APL. The need to

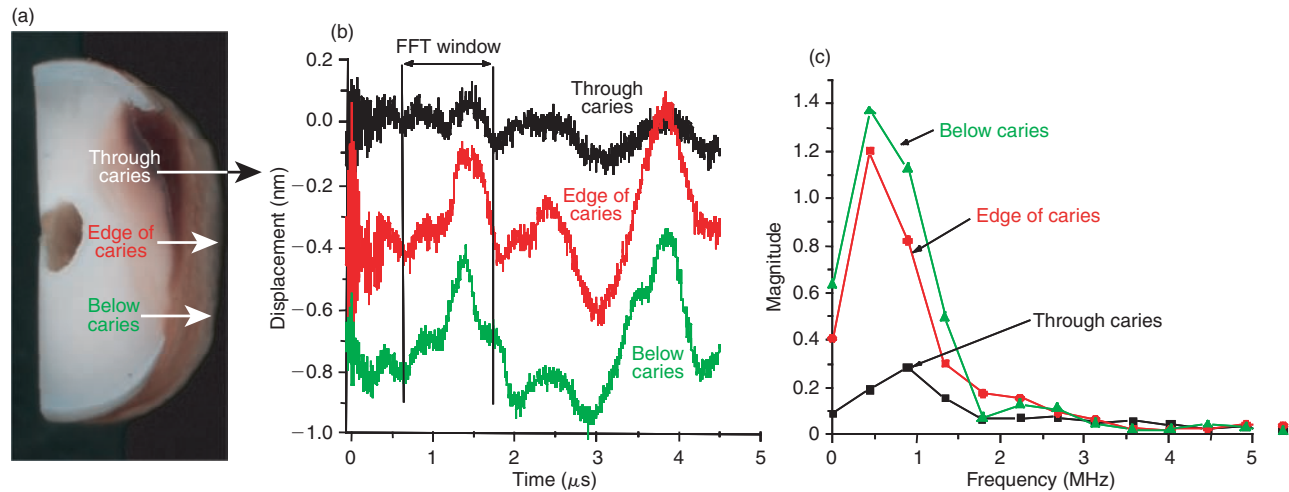


Figure 11. The use of surface waves for the detection of caries. (a) Locations of generation (red) and detection (green) of surface waves. (b) Measured and (c) corresponding frequency spectra of the windowed portion.³⁵

characterize the fundamental properties (both mechanical and optical) of window materials is an important role that the Laboratory plays for the military. Other optical window materials of interest include AION and spinel, which are being investigated for various transparent armor systems.³⁷ These materials hold promise for low-cost, high-strength combat vehicle vision blocks, aircraft blast shields, soldier eye/face protection, and ground vehicle windows.

Support of the Space Department has occurred over many different programs. In addition to the investigation of the solar panels presented here, APL has used LBU to assess the bond integrity of SiC bars to be used on a telescope for the LONg-Range Reconnaissance Imager (LORRI) program and the mechanical properties of various baffle materials.

Finally, LBU has shown promise in delivering the type of valuable information needed for clinical dentistry. Measurements have shown LBU to be sensitive to early stages of surface caries and the presence of various bulk defects. As mentioned previously, laser ultrasonics is far from the solution to every material characterization problem, but it unquestioningly does have its place in solving traditionally difficult problems.

REFERENCES

- ¹Shull, P. (ed.), *Nondestructive Evaluation: Theory, Techniques, and Applications*, Marcel Dekker Inc., New York (2002).
- ²Scruby, C. B., and Drain, L. E., *Laser Ultrasonics: Techniques and Applications*, Adam-Hilger, New York (1990).
- ³White, R. M., "Generation of Elastic Waves by Transient Surface Heating," *J. Appl. Phys.* **34**(12), 3559–3567 (1963).
- ⁴Scruby, C. B., Dewhurst, R. J., Hutchins, D. A., and Palmer, S. B., "Quantitative Studies of Thermally Generated Elastic Waves in Laser-Irradiated Metals," *J. Appl. Phys.* **51**(12), 6210–6216 (1980).
- ⁵Wagner, J. W., "Optical Detection of Ultrasound," in *Physical Acoustics* **19**, W. P. Mason and A. D. Pierce (eds.), Academic Press, New York, pp. 201–266 (1990).

- ⁶Spicer, J. B., and Wagner, J. W., "Absolute Calibration of Interferometric Systems for Detection and Measurement of Surface Acoustic Waves," *Appl. Optics* **27**(16), 3561–3566 (1988).
- ⁷Murray, T. W., *Laser Interactions with Materials: Optimizing the Laser Source for the Generation of Acoustic Waves in Laser Ultrasonics Applications*, Ph.D. Dissertation, The Johns Hopkins University, Baltimore, MD (1997).
- ⁸Harris, D. C., *Materials for Infrared Windows and Domes: Properties and Performance*, SPIE Press, Bellingham, WA (1999).
- ⁹Harris, D. C., "Overview of Sapphire Mechanical Properties and Strategies for Strengthening Sapphire," in *Proc. 7th DoD Electromagnetic Windows Symp.*, pp. 310–318 (1997).
- ¹⁰Auld, B. A., *Acoustic Fields and Waves in Solids, Vol. I*, Krieger Publishing Company, Malabar, FL (1990).
- ¹¹Nye, J. F., *Physical Properties of Crystals: Their Representation by Tensors and Matrices*, Clarendon Press, Oxford, UK (1992).
- ¹²Papadakis, E. P., "Ultrasonic Velocity and Attenuation: Measurement Methods with Scientific and Industrial Applications," in *Physical Acoustics XII*, W. P. Mason and N. Thurston (eds.), Academic Press, New York, pp. 277–374 (1976).
- ¹³Vary, A., *Material Analysis by Ultrasonics: Metals, Ceramics, Composites*, Noyes Data Corp., NJ (1987).
- ¹⁴Papadakis, E. P., Lynnworth, L. C., Fowler, K. A., and Carnevale, E. H., "Ultrasonic Attenuation and Velocity in Hot Specimens by the Momentary Contact Method with Pressure Coupling, and Some Results on Steel to 1200°C," *J. Acoust. Soc. Am.* **52**(3), 850–857 (1972).
- ¹⁵Blodgett, D. W., Baldwin, K. C., and Spicer, J. B., "Measurement of High Temperature Elastic Moduli of Infrared Transparent Materials," in *Proc. IRIS Specialty Group Mtg. on Materials and Detectors* (1998).
- ¹⁶Blodgett, D. W., Baldwin, K. C., Thomas, M. E., and Spicer, J. B., "Measurement of High Temperature Elastic Moduli of Infrared Dome Materials," in *Proc. 7th DoD Electromagnetic Windows Symp.* (1998).
- ¹⁷Blodgett, D. W., and Baldwin, K. C., "High-Temperature Mechanical Characterization of Single-Crystal Sapphire Using Laser-Based Ultrasonics," in *Proc. SPIE AeroSense Conf.* (Apr 1999).
- ¹⁸Blodgett, D. W., "Elastic Moduli and Defect Orientation Studies of Aspen-Treated Sapphire Using Laser Ultrasonics," in *Proc. 8th DoD Electromagnetic Windows Symp.* (2000).
- ¹⁹Duncan, D. D., Baldwin, K. C., Blodgett, D. W., Elko, M. J., Joseph, R. I., et al., "Experimental and Theoretical Assessment of Mechanical and Optical Effects in Non-Uniformly Heated IR Windows," *Johns Hopkins APL Tech. Dig.* **22**(3), 394–408 (2001).
- ²⁰Regan, T. M., Harris, D. C., Blodgett, D. W., Baldwin, K. C., Miragliotta, J. A., et al., "Neutron Irradiation to Increase the C-Axis Compressive Strength of Sapphire at Elevated Temperatures," *SPIE*, pp. 338–355 (2001).

- ²¹Regan, T. M., Harris, D. C., Blodgett, D. W., Baldwin, K. C., Miragliotta, J. A., et al., "Neutron Irradiation of Sapphire for Compressive Strengthening II. Physical Property Changes," *J. Nucl. Materials* **300**, 47–57 (2002).
- ²²Goto, T., Andersen, O. L., Ohno, I., and Yamamoto, S., "Elastic Constraints of Corundum up to 1825 K," *J. Geophys. Res.* **94**(86), 7588–7602 (1989).
- ²³Hahn, D. V., Baldwin, K. C., Blodgett, D. W., and Lazarevich, A. K., "Preliminary Analysis of Hazed Solar Cells on the MESSENGER Flight Panel," A1F(5)03-U-114, JHU/APL, Laurel, MD (2003).
- ²⁴Miserendino, L. J., and Pick, R. M., *Lasers in Dentistry*, Quintessence Books, Chicago, IL (1995).
- ²⁵Avery, J. K., *Essentials of Oral Histology and Embryology: A Clinical Approach*, Mosby, St. Louis, MO (2000).
- ²⁶Barber, F. E., Lees, S., and Lobene, R. R., "Ultrasonic Pulse-Echo Measurements in Teeth," *Arch. Oral Biol.* **14**, 745–760 (1969).
- ²⁷Baum, G., Greenwood, I., Slawski, S., and Smirnov, R., "Observation of Internal Structures of Teeth by Ultrasonography," *Science* **139**, 495–496 (1963).
- ²⁸Kossoff, G., and Sharpe, C. J., "Examination of the Contents of the Pulp Cavity in Teeth," *Ultrasonics* **4**, 77–83 (1966).
- ²⁹Reich, F. R., Brenden, B. B., and Porter, N. S., *Ultrasonic Imaging of Teeth*, Battelle Memorial Inst., Pacific Northwest Laboratory, Richland, WA (1967).
- ³⁰Ng, S. Y., Ferguson, M. W. J., Payne, P. A., and Slater, P., "Ultrasonic Studies of Unblemished and Artificially Demineralized Enamel in Extracted Human Teeth: A New Method for Detecting Early Caries," *J. Dent.* **18**, 201–209 (1987).
- ³¹Peck, S. D., Rowe, J. M., and Briggs, G. A. D., "Studies on Sound and Carious Enamel with the Quantitative Acoustic Microscope," *J. Dent. Res.* **68**, 107–112 (1998).
- ³²Blodgett, D. W., "Ultrasonic Assessment of Tooth Structure," in *Proc. SPIE Laser Tissue Interaction XIII*, pp. 284–288 (2002).
- ³³Blodgett, D. W., "Applications of Laser-Based Ultrasonics to the Assessment of Tooth Health" *J. Acoust. Soc.* **114**(1), 543–549 (2003).
- ³⁴Blodgett, D. W., and Massey, W., "Dental Hard Tissue Characterization Using Laser Based Ultrasonics," in *Proc. SPIE Laser Tissue Interaction XIV*, pp. 226–231 (2003).
- ³⁵Blodgett, D. W., and Baldwin, K. C., "Assessment of Tooth Health Using Laser Based Ultrasonics," in *Proc. SPIE Laser Tissue Interaction XI*, pp. 588–598 (2000).
- ³⁶Lertchirakarn, V., Palamara, J. E. A., and Messer, H. H., "Anisotropy of Tensile Strength of Root Dentin," *J. Dent. Res.* **80**(2), 453–456 (2000).
- ³⁷Gilde, G., Patel, P., Blodgett, D., and Hahn, D., "Evaluation of the Hot Isostatic Pressing Parameters on the Optical Properties of Spinel," in *Proc. Electromagnetic Windows Symp.* (2004).

ACKNOWLEDGMENTS: The work outlined in this article has been supported through the years by many organizations and individuals. Investigations into the mechanical properties of sapphire were funded in part by the APL IR&D program and through Dr. Dan Harris (NAWC). The APL Office of Technology Transfer and the Air Defense Systems Department supported the dental studies. In addition, we would like to acknowledge Dr. Ward Massey of the Baltimore College of Dental Surgery and Dr. Christopher Longbottom of the University of Dundee for many helpful discussions and for providing the extracted teeth used for this study. Finally, we would like to acknowledge Daniel Hahn and Alison Lazarevich for their valuable laboratory assistance.

THE AUTHORS

David W. Blodgett and Kevin C. Baldwin were co-collaborators on the work reported in this article. Dr. Blodgett, a member of APL's Principal Professional Staff, received a B.S.E.E. from Purdue University in 1991 and an M.S. and Ph.D. from The Johns Hopkins University in 1995 and 1998, respectively. Since joining the Electro-Optical Systems Group of the Air Defense Systems Department (ADSD) in 1991, he has been involved with a number of programs, including the characterization of the temperature-dependent optical and mechanical properties of optical window materials, assessment of tooth health using laser ultrasonics, and detection of low-level rebar delamination in reinforced concrete structures. His current research activities range from the analysis, design, and simulation of optical synthetic aperture lidar systems to the development of vibrometer systems for health monitoring of machines and structures. Dr. Baldwin received B.S. and M.S. degrees in optics in 1990 and 1991, respectively, from the University of Rochester; an M.S. in electrical engineering from the Rochester Institute of Technology; and an M.S.E. in 1994 and Ph.D. in 1998, both in electrical engineering, from The Johns Hopkins University. Dr. Baldwin is also a member of ADSD's Electro-Optical Systems Group. He has worked on a number of projects ranging from the design of low F/# IR imaging systems to the modeling, developing, and testing of underwater imaging systems. Currently, his activities range from the simulation of synthetic aperture lidar systems to 3-D imaging of historical artifacts. While his research pursuits are quite varied, central to these activities is the rapid development of computer-controlled systems based on COTS technology. The authors can be reached through David Blodgett. His e-mail address is david.blodgett@jhuapl.edu.



David W. Blodgett



Kevin C. Baldwin